



Flexural Strength Prediction in FRP Strengthened Concrete Bridge Girders

Muruganandam Mohanamurthy¹ and Nur Yazdani²

¹Structural Engineer – II, Parsons Brinckerhoff, Baltimore, MD 21201, USA

²Department of Civil Engineering, University of Texas at Arlington, Arlington, Texas 76019, USA
yazdani@uta.edu

ABSTRACT

Fiber Reinforced Polymer (FRP) composite material wraps provide effective and economic solution for rehabilitating and upgrading of existing reinforced and precast concrete bridge structures with damage or deterioration, and is being used by many highway departments. This study consisted of the review and comparison of relevant design guidelines and standards for FRP wrap strengthening of damaged concrete bridge elements, both from U.S.A. and abroad. Based on the flexural load carrying capacity of a prestressed bridge girder and possible failure modes, the various design provisions were validated against experimental results from literature and finite element analysis. FRP rupture, the preferred failure flexural mode, is validated in both experimental and theoretical analysis. In general, the code and practice guidelines are quite conservative in predicting the flexural strength of AASHTO type bridge girders with FRP wrapping. FRP strengthening design provisions are recommended based on the comparative study.

Key words: FRP wraps, Bridge strengthening, Bridge repair, FRP design guides, flexural capacity

INTRODUCTION

The infrastructure report card for U.S.A. states that over 11% of the nation's 607,380 bridges are structurally deficient and an estimated \$20.5 billion is required annually to upgrade the nation's deficient bridges by the year 2028 [1]. However, the current annual expenditure for bridge investments is only \$12.8 billion and an additional \$8 billion is required annually to upgrade the nation's deficient bridges. Feasible bridge retrofitting and rehabilitation is, therefore, a viable option for upgrading deficient bridges, address budget constraints and reduce construction times. Fiber Reinforced Polymer (FRP) strengthening is one such method that can increase the life of a bridge and reduce the cost for replacement. The state highway departments have to handle a considerable number of concrete bridges that are damaged due to vehicle or vessel collision, reinforcing steel corrosion or fire. Over height vehicles collisions due to low clearance of older bridges or increase of roadway overlay thickness is the primary cause of the first type of damage [2]. In the last decade, strengthening of damaged bridge girders was in some cases achieved by adding additional steel plates. This method has some disadvantages, such as transportation, handling, and installing heavy plates and corrosion of plates [3]. Fiber Reinforced Polymer (FRP) strengthening has been a popular, economic and convenient method for restoring and enhancing the strength and stiffness of damaged concrete bridges since 1999 [4, 5]. Fig. 1 shows a damaged concrete bridge girder before and after the FRP strengthening process.

FRP wrapping can improve flexural, shear, axial, and torsional strengths, and also the serviceability of existing or damaged bridges. Due to the changes in traffic volume and increasing truck loads, if bridges need to be upgraded to carry the additional load, FRP strengthening can be conveniently utilized for this purpose. Recent developments in finite element software have allowed the effective modeling of FRP strengthened prestressed concrete bridge girders [6]. A survey was conducted by the authors herein of the state highway departments to find the various concrete bridge retrofitting techniques that each department is using. It was found that FRP strengthening technique for concrete bridges is quite popular and expanding. A total of 24 highway departments are currently using FRP laminate application as a bridge retrofitting technique. The corresponding states are: Alabama, California, Colorado, Florida, Hawaii, Idaho, Indiana, Iowa, Kansas, Louisiana, Michigan, Missouri, Nebraska, Nevada, New Jersey, New Mexico, New York, North Carolina, Oregon, Pennsylvania, South Dakota, Texas, Washington and Wisconsin. Some other states are considering the adoption of this technique.

FRP is a composite material manufactured in the form of polymer matrix reinforced with fibers. Common available fibers are glass, carbon, or aramid, and polymers made up of epoxy, vinyl ester or polyester. FRP composite wrapping is a highly promising structural strengthening process and has been successfully used. FRP wrapping has more advantages than adding reinforcement or steel plates to increase the strength of structures; it is lighter in weight, non-corrosive in nature and has a significant load capacity. The installation of FRP laminates is faster, simpler and less labor intensive, compared to adding structural steel or casting additional reinforced concrete. Use of FRP wrapping for in-service bridge strengthening is economic and fast, where prolonged construction times may lead to transportation disruptions and associated economic losses and mass inconvenience.

This article presents the design and development of two topologies working at single and dual frequencies. Single frequency approach operating at 7.3 GHz with inset feed antenna and dual-band operated switched beam system working at 7.0/8.1GHz are detailed and both are implemented on high resistivity silicon substrate. Design of individual circuits like hybrids, phase shifters, cross coupler, patch antennas are detailed and further integrated to realize broadband Butler matrix. Complete switched beam assemblies are realized after incorporating patch antennas at desired frequencies. Design details of the realized assemblies along with the experimental results are detailed in this article.



Fig. 1 Damaged and Strengthened Girders

RESEARCH SIGNIFICANCE

Several design guides, standards and manufacture's guidelines are available for the design and analysis of FRP strengthening systems for concrete structures. Some of these provisions are based on theoretical models, while others are based on experimental work. The material and mechanics models used by the various guides are quite different in some cases. A comparative study was performed herein to evaluate the strength predictions from these models so that the users have a basis of choosing an appropriate model.

Investigation of the prediction accuracy (from various available models) based on flexural load capacity, crack pattern, and failure modes using an available non-linear finite element program was undertaken herein. The analytical results were then compared with the results from a previous experimental study in order to determine the relative accuracy of each analytical procedure. Based on these comparisons, an appropriate code-based design procedure for FRP strengthening of prestressed concrete bridge girders was recommended.

REVIEW OF CURRENT DESIGN PRACTICE

Several standards and guidelines for FRP strengthening of concrete structures from U.S and other countries were located after a through literature review, and are listed in [7-14]. When FRP strengthening was first adopted by highway departments, some of them used the FRP manufacture's guidelines to estimate FRP system strengths, because there were no other available guidelines. In 1998, the MBrace guide was developed by the BASF chemical company, and it has been used since then by some highway departments. BASF recently discontinued the MBrace guide and currently recommends the ACI 440 guidelines. The FIB report was published in 2011. In 2002, ACI published the first edition of the FRP strengthening design guide; it was developed based on the MBrace guide. The second edition of the guide was published in 2008. Other guides were published in Canada [11] and Italy [9]. In U.K., the TR55 technical report was published first in 2000, with subsequent upgrades. AASHTO published the first edition of its guide specifications in 2012, based on NCHRP 655 and NCHRP 688 reports [7, 13, 15].

Each publication specifies partial factors of safety, characteristic and design values of material properties and strength reduction factors. For flexural strength determination, generally the trial and error method is followed to estimate the neutral axis of the FRP strengthened structures, in the absence of any direct method. Different interpolation methods are employed to calculate the concrete compression stress block parameters; this may result in differences in predicted strengths.

In ACI 440, the design recommendations are based on limit state method and ACI 318 [16] strength and serviceability requirements. Additional load factors are applied to the contribution of the FRP reinforcement. These factors were determined based on statistical evaluation of variability in mechanical properties, predicted versus full-scale test results, and field evaluations. FRP related reduction factors were calibrated to produce reliability indices typically above 3.5.

In AASHTO 2012, the provisions are limited to concrete compressive strengths not exceeding 55 MPa. The consideration of service limit states, strength limit states, extreme event limit states and fatigue limit state load combinations are considered as per AASHTO LRFD provisions [17].

In FIB 14, design calculations are based on analytical or empirical models. Design procedure consists of a verification of both serviceability limit state and ultimate limit state. Material partial safety factors are used to estimate structural strength.

In TR 55, the flexural strength equation is based on the parabolic-rectangular-stress-strain relationship for concrete in compression. Partial safety factors for concrete or reinforcement are calculated based on design situations. It is also possible in some situations for the ultimate strain in the FRP to govern failure of a strengthened structure.

In CNR 2004, strength and strain properties of FRP materials used for strengthening, as well as those of existing materials, are described by the corresponding characteristic values. The flexural analysis of FRP strengthened members can be performed by using strain compatibility and force equilibrium. The stress at any point in a member must correspond to the strain at that point; the internal forces must balance the external load effects.

In ISIS Canada, there are four potential flexural failure modes for externally-strengthened reinforced concrete flexural members. These are: concrete crushing before yielding of the reinforcing steel, steel yielding followed by concrete crushing, steel yielding followed by FRP rupture and de-bonding of the FRP reinforcement at the FRP/concrete interface.

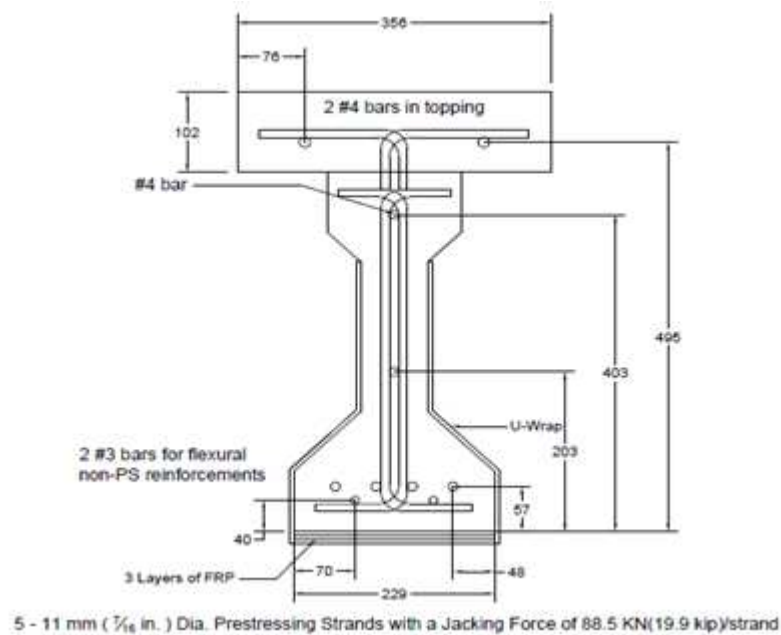


Fig. 2 Experimental Prestressed Girder Cross Section

PREVIOUS EXPERIMENTAL STUDY

The literature review undertaken herein located a previous experimental program against which the theoretical analyses performed herein could be compared. The experimental work involved half scale AASTHO prestressed concrete Type II girders and composite decking that was flexurally repaired with CFRP [18]. The girders had an average concrete compressive strength of approximately 69 MPa, five low-relaxation grade 270 seven-wire prestressing strands and three 345 MPa strength non-prestressed rebars. One of the strands was supposed to be broken in practice. An additional 102 mm thick decking with two rebars was cast on top to simulate a composite section. Fig. 2 shows the cross-section and the reinforcement details, including the CFRP arrangements. Two or three layers of longitudinal CFRP 5.2 m in length were provided at the bottom of the girder for flexural strengthening. For shear strengthening, 305 mm wide CFRP strips were used as transverse U-wraps (one wrap only) that extended up to the girder web, as shown. Eight CFRP strengthened girders were tested, five with two layers of flexural CFRP strengthening and the remaining three with three layers of flexural CFRP.

Table 1 presents the material properties for the CFRP used in the experiments. Typical dry fiber properties values given are based on ASTM test results. The composite gross-laminate properties of FRP system is calculated using the total cross-sectional area of the cured FRP system, including all fibers and resin [8]. Fig. 3 shows the test setup used in the experiment. The four point static loading was applied using a 2224 kN load actuator, and corresponding load and deflections were noted. The pertinent experimental results are presented in Table 2. All girders failed by the CFRP rupture mode, which is the preferred mode of failure according to the design guidelines.

Table -1 Properties of One Layer of CFRP Material

CFRP Properties	Typical Dry Fiber Properties	*Composite Gross Laminate Properties (one layer)
Tensile Strength	3.79 GPa	834 MPa
Tensile Modulus	230 GPa	82 GPa
Ultimate Elongation	1.7%	0.85%
Density	1.74 g/cm ³	N/A
Weight per sq. yd.	644 g/m ²	N/A
Rupture strain	0.012	0.012
Nominal Thickness	N/A	1.0 mm

*Gross laminate design properties are calculated based on ACI 440.

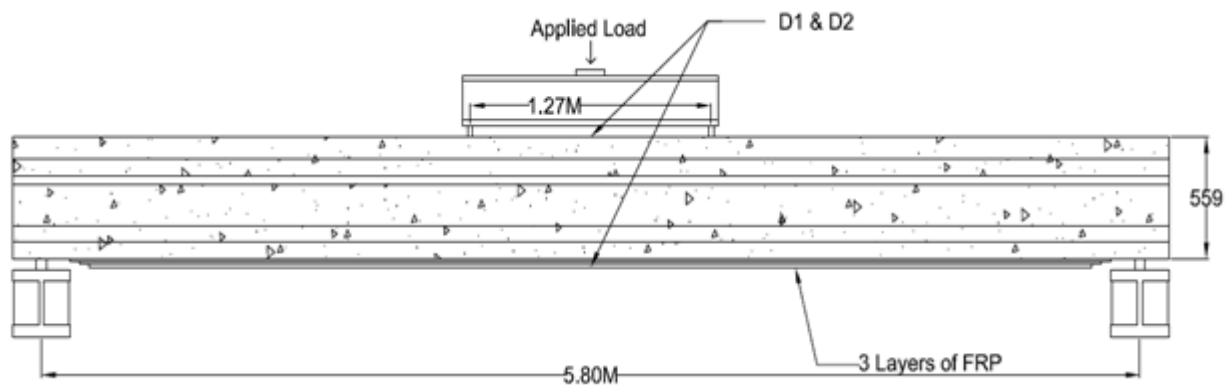


Fig.3 Static loading test setup

Table -2 Experimental Results

Girder Group	Average Flexural Failure Load (kN)	Flexural Failure Load Range (kN)	Average Maximum Deflection (mm)	Maximum Deflection Range (mm)
Five girders with two CFRP layers	372	344 – 401	50	40 – 62
Three girders with three CFRP layers	451	441 – 464	63	58 – 70

FINITE ELEMENT MODELING (FEM)

ANSYS 14.5 version [19] was used herein to theoretically model the experimental girders for comparison purposes. Both the girder groups with two and three layers of CFRP were modeled herein. SOLID65, an ANSYS element for 3-D models of concrete structures, was used. Link180 elements were used for discrete reinforcement and Shell141 for both the CFRP wrapping and epoxy. Table 3 and 4 present the geometric and material properties used in the FEM, respectively. An optimum mesh size of 38 × 51 × 152 mm was used herein. The FRP layers were assumed to be perfectly bonded to the concrete surface, and the epoxy layer between the FRP and the concrete was ignored. This is because the experimental girders failure occurred due to FRP rupture, not due to FRP delimitation. A nonlinear analysis was performed herein to capture the concrete crack pattern from initial stage to failure stage. Details of the FEM are available in the literature [20].

Table -3 ANSYS Geometric Properties

ANSYS Element	Properties		
Link180	Cross-Sectional Area, mm ²	Prestressing strand	74
		#3 Steel rebar	71
		#4 Steel rebar	129
Solid65	Material Number	Concrete	0
	Volume Ratio		0
	Orientation Angle		0
Shell41	Thickness, mm	FRP	1.0
Solid185	ANSYS standard values	Steel Plate	N/A

Fig. 4 shows the progression of crack patterns at various steps in the FEM, and also the extensive cracking at failure in the girder model with three CFRP layers (step 12). The load associated with this step represented the flexural capacity of the FRP strengthened model. In the experimental study, only the maximum deflection value at failure was recorded. The final deflection values of 46 and 58 mm from the FEM for 3-layer and 2-layer CFRP girders, respectively, are slightly lower than the average corresponding experimental values of 50 and 63 mm. The 8% difference shows that the FEM models were slightly stiffer than the experimental girders. The possible reason is that the FEM assumes a perfect bond between concrete and steel, and achieving such perfection in an experiment is very difficult. Another reason could be the size of the mesh used in the FEM. A smaller mesh size than the one used in the FEM could possibly yield a more accurate result. Fig. 5 shows the FEM strain values in one of the flexural CFRP laminates at the time of failure. The maximum rupture strain of the FRP used in the experimental girder was 0.012 (Table 1), closely matching the experimental result. From the crack patterns, strain comparison and deflections, it is clear that the FEM supported the FRP rupture flexural failure mode observed in the experimental girders. Table 5 presents a comparison of the deflections from the FEM with those from hand calculations. The values are very close, validating the accuracy of the FEM.

Table -4 ANSYS Material Properties

Material	Properties		
Prestressing strand, MPa	Linear Isotropic	Elastic Modulus	18.9×10^4
		Poisson's Ratio	0.3
Mild steel rebar, MPa	Linear Isotropic	Elastic Modulus	19.9×10^4
		Poisson's Ratio	0.3
	Bilinear Isotropic	Yield Stress	4130
		Tangent Modulus	4130
Concrete	Density	Dens	2400 kg/m^3
	Linear Isotropic	Elastic Modulus	$3.9 \times 10^4 \text{ MPa}$
		Poisson's Ratio	0.25
	Concrete	Open Shear Transfer Coefficient	0.3
		Closed Shear Transfer Coefficient	1
		Uniaxial Cracking Stress	750
		Uniaxial Crushing Stress	-1
FRP	*Linear Orthotropic	Elastic Modulus, E_x	82,000 MPa
		Elastic Modulus, E_y	4800 MPa
		Elastic Modulus, E_z	4800 MPa
		Poisson's Ratio, PR_{xy}	0.22
		Poisson's Ratio, PR_{yz}	0.22
		Poisson's Ratio, PR_{xz}	0.30
		Shear Modulus, G_y	3200 MPa
		Shear Modulus, G_{xy}	3200 MPa
		Shear Modulus, G_{xy}	1800 MPa

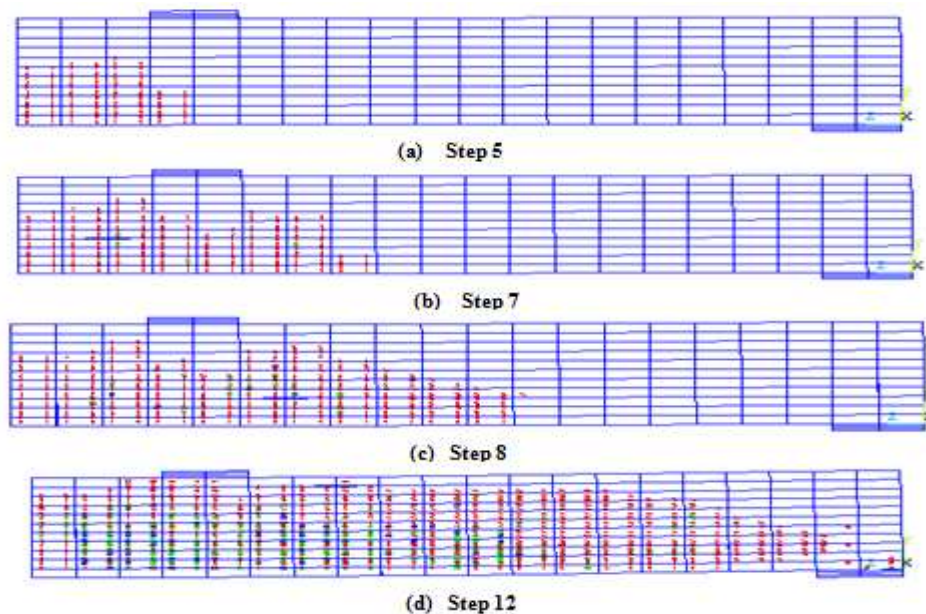


Fig.4 Crack pattern variations in FEM due to load increments

Table- 1 Deflection Checks (Girder with two flexural CFRP layers)

	FEM	Hand Calculation
Deflection due to prestress	-5.9 mm	-6.0 mm
Deflection due to self-weight and prestress	-5.6 mm	-5.7 mm

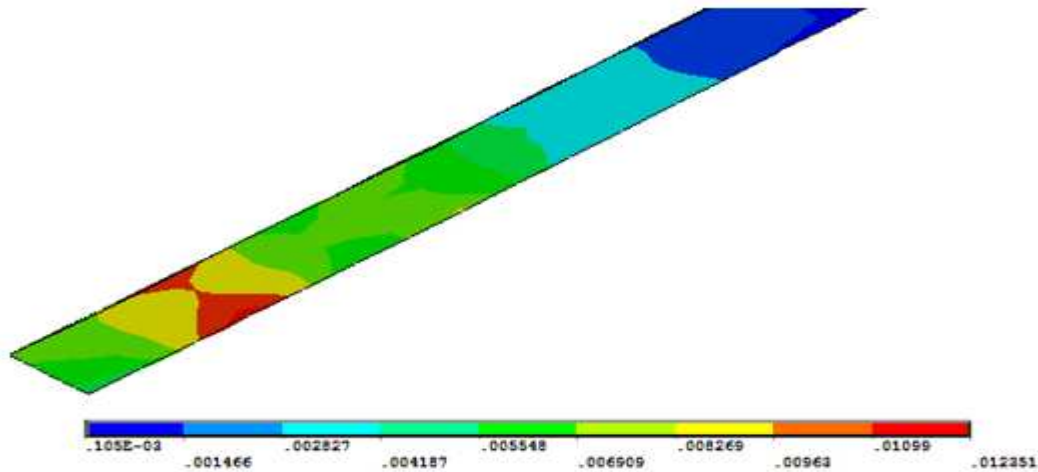


Figure 1: FRP Bottom Layer Strain Distribution in FEM at Failure

COMPARISON AMONG DESIGN GUIDELINES

Different flexural strength equations are recommended by the identified codes and guidelines for FRP strengthening, as discussed above. All the publications listed herein include a term for the FRP laminate strength, as an additional quantity to the prestressing and mild steel flexural capacities. They also assume linear strain distributions up to failure, and a concentrated tensile force provided by the FRP wrapping. Parabolic distribution of concrete compressive stress is also common, with associated rectangular equivalent compressive stress block. There are some variations in the specification of the centroid of the parabolic stress distribution, the width of the equivalent stress block and the checking thresholds for the various flexural failure modes. In general, the following failure modes are considered: (1) Crushing of concrete in compression before yielding of the reinforcing steel; (2) Yielding of the tension steel followed by rupture of the FRP laminate; (3) Yielding of the tension steel followed by concrete crushing; (4) Shear/tension delamination of the concrete cover; and (5) Debonding of the FRP from the concrete substrate.

To compare the flexural strength predictions from the different sources, the flexural design load capacities for the experimental girders discussed previously were calculated herein using the various guideline equations. The average values, together with the average experimental and the FEM flexural load capacities are shown in Table 6. A detailed worked out example for the experimental girder strength with two CFRP layers, and using the ACI 440 provisions, is presented in App. A. The example will be a good review source for readers, and it shows how the various numbers in Table 6 were calculated.

The assumed concrete compressive stress distributions vary among the different guidelines, and this results in minor variations in the corresponding load capacities. Other possible reasons for this variation are calculation procedure of neutral axis in the moment calculations and different partial safety factors in the various codes. The guidelines produce flexural capacities that have a wide range of 378 – 472 kN for girders with two CFRP layers, and 446 – 580 kN for those with three CFRP layers. All guidelines, experimental results, and FEM resulted in failure modes that are initiated by FRP rupture, which is the preferred mode that utilizes the full capacity of the FRP. The code provisions allow for design moment calculations for other possible failure mode types as well, and they specify checks to consider or eliminate various failure modes. The average of all failure load predictions from the guidelines is 419 kN for girders with two CFRP layers, and 503 kN for girders with three CFRP layers. It appears that these values are a bit non-conservative, if they are compared to the experimental values and FEM predictions, as seen in Table 6. The experimental values are around 5% lower than the FEM values, showing again the slightly stiffer nature of the FEM. The averages from the guideline predictions are around 10% higher than the experimental results. All flexural capacities from guidelines are greater than the experimental results, except for the FIB 14 prediction with 3 layers of CFRP. The ACI, FIB 14, TR55 and CNR guidelines are more in line with the theoretical and experimental results for the girder load capacity, ACI being the closest overall. MBrace has discontinued the design guideline for FRP strengthening and is currently recommending ACI 440. In consideration of these factors, the ACI 440 guidelines seem to be the best predictor of the flexural capacity of a typical AASHTO type bridge girder with CFRP strengthening.

Table 2: Flexural Load Capacities of Strengthened Girders Three Point Loading on 5.8 m Simple Span

	Average Flexural Load Capacity (kN)	
	2 CFRP layers (five girders)	3 CFRP layers (three girders)
FEM	395	474
Experimental (ElSafty and Graeff, 2012)	372	451
ACI 440	394	469
AASHTO	472	580
FIB 14	378	446
ISIS	463	532
TR55	384	465
Mbrace	458	563
CNR	383	467

Limitations

The various guidelines considered in this study provide procedures for finding the flexural, shear, and axial capacities of FRP strengthened members. This study is limited to investigation of flexural capacities due to FRP rupture only.

CONCLUSIONS AND RECOMMENDATIONS

The following conclusions may be based on the findings from this study:

- Many U.S. highway departments have adopted FRP strengthening as an option for rehabilitating damaged highway concrete bridge elements.
- A number of design codes, standards and guidelines are available worldwide that deal with FRP strengthening of concrete structures. They contain equations for the prediction of flexural, shear, axial and torsional strengths of such strengthened structures. Some of these documents contain different stress distributions for the flexural strength determination and it results in variations in capacity predictions.
- ANSYS 14.5 version software is capable of predicting crack patterns, failure mode and flexural load capacity in a FRP strengthened girder. This is evident from the validation of the finite element model results with the experimental results. The difference between experimental and the theoretical results was around 5%.
- Experimental and FEM procedures both resulted in failure of the subject girder due to FRP rupture, which the desired mode and is recommended by all identified guidelines. The maximum flexural load capacity for a FRP strengthened girder was obtained through the AASHTO 2012 guidelines, and the minimum through the FIB guidelines. The variations in load capacities are substantial.
- Various design standards are quite conservative in predicting the flexural load capacity of a FRP strengthened AASHTO girder.

It is recommended that the ACI guidelines be followed for designing FRP strengthening systems for concrete bridges. The ACI guidelines are reasonable and predict strength values that are consistent with the theoretical and experimental results.

APPENDIX

Sample Example for Flexural Capacity Calculation

The following example calculates the flexural load capacity for the experimental girder with three CFRP flexural strengthening layers. ACI 440 provisions are applied herein.

Girder Details

Compressive strength of concrete $f'_c = 69 \text{ MPa}$
 Ultimate strength of strands = 1862 MPa
 No. of 11 mm diameter undamaged strands = 4
 Yield strength of mild steel $f_y = 414 \text{ MPa}$
 Area of girder = 94838 mm²
 Moment of inertia = $3.4 \times 10^9 \text{ mm}^4$
 Distance from girder top to the prestress centroid $d_p = 457 \text{ mm}$
 Distance from girder top to the CFRP centroid $d_f = 559 \text{ mm}$
 $d_s = 508 \text{ mm}$ $Y_b = 305 \text{ mm}$

CFRP Physical Properties

Thickness per CFRP layer $t_f = 1.016 \text{ mm}$
 Ultimate tensile strength of CFRP $f_{fu} = 834 \text{ MPa}$
 CFRP rupture strain $[\epsilon]_{fu} = 0.22$
 Modulus of elasticity of CFRP layers $E_f = 82048 \text{ MPa}$

Step 1 – Calculate the CFRP System Design Material Properties

The girder is located in an exterior exposure condition and a CFRP material will be used. Therefore, per ACI 440, an environmental reduction factor of 0.85 is used.

$$\text{Modified CFRP ultimate strength } f_{fu} = C_E f_{fu} = 0.85(121) = 709 \text{ MPa}$$

$$\text{Modified CFRP strain } \varepsilon_{fu} = C_{E\varepsilon fu} = (0.85)(0.0085) = 0.0072$$

Step 2 – Preliminary Calculations**Properties of Concrete:**

Strength modifier, β_1 , from ACI 318-11, section 10.2.7.3 = 0.65

$$\text{Concrete Modulus, } E_c = 57000\sqrt{f'_c} = 57,000\sqrt{10000}\text{psi} = 39300 \text{ MPa}$$

Properties of the Prestressing Steel

$$\text{Area of prestressing strands } A_{ps} = 297 \text{ mm}^2$$

$$\text{Modulus of steel } E_{ps} = 189605 \text{ MPa}$$

Properties of CFRP

$$\text{Area of CFRP wraps } A_f = (3 \text{ plies})(0.1016 \text{ cm/ply})(22.86 \text{ cm}) = 6.97 \text{ cm}^2$$

$$\text{Modulus of CFRP, } E_f = 82048 \text{ MPa}$$

Section Properties:

$$\text{Area of girder } A_{cg} = 94,838 \text{ mm}^2$$

$$\text{Distance to girder } cg \text{ from top } y_t = 254 \text{ mm}$$

$$\text{Moment of inertia of girder } I_g = 3.4 \times 10^9 \text{ mm}^4$$

$$\text{Radius of gyration } r = 1890 \text{ mm, Effective prestress } f_{pe} = 827 \text{ MPa}$$

$$\text{Strain for effective prestress } \varepsilon_{pe} = 120/27500 = 0.0044$$

$$\text{Effective prestress force } P_e = 0.46 \times 120 = 245.5 \text{ kN}$$

$$\text{Eccentricity of prestressive force } e = dp - yt = 18 - 10 = 203 \text{ mm}$$

Step 3 – Determine the existing state of strain on the soffit

The existing state of strain is calculated assuming the girder is uncracked and the only loads acting at the time of FRP installation are dead loads.

MDL = 2.96 kN – m (kN · m ?), maximum dead load moment with the girder self – weight and slab.

$$\text{Initial strain in the beam soffit: } \varepsilon_{bi} = \frac{-P_e}{E_c A_{cg}} \left(1 + \frac{ey_b}{r^2}\right) + \frac{M_{DL} y_b}{E_c I_g} = -0.0001$$

Step 4 – Determine the design strain of the CFRP system

The strain in the CFRP, accounting for deboning failure mode, is:

$$\varepsilon_{fd} = 0.083 \sqrt{\frac{f'_c}{n_f E_{ft} f}} = 0.0069 \geq 0.9 \varepsilon_{fu} = 0.0069 \geq 0.0065 \text{ where deboning does not control.}$$

$$\text{So, } \varepsilon_{fd} = 0.0065$$

CFRP rupture mode controls, as preferred.

Step 5 – Estimate c, the depth to the neutral axis

Assume a reasonable initial value of c = 102 mm.

Step 6 – Determine the efficiency level of strain in the CFRP reinforcement

$$\varepsilon_{fe} = 0.003 \left(\frac{d_p - c}{c}\right) - \varepsilon_{bi} = 0.013 \leq \varepsilon_{fd} = 0.0065.$$

$$\text{So, assume } \varepsilon_{fe} = 0.0065$$

Step 7 – Calculate the strain in the existing prestressing steel and regular steel:

$$\varepsilon_{pnet} = (\varepsilon_{fe} + \varepsilon_{bi}) \left(\frac{d_p - c}{d_f - c}\right) = 0.0052, \text{ net tensile strain in the prestressing steel beyond decompression.}$$

$$\text{Prestress strain, } \varepsilon_{ps} = \varepsilon_{pe} + \frac{P_e}{A_c E_c} \left(1 + \frac{e^2}{r^2}\right) + \varepsilon_{pnet} = 0.0097 \leq 0.035, \text{ ok.}$$

$$\text{Regular steel strain, } \varepsilon_s = (\varepsilon_{fe} + \varepsilon_{bi}) \left(\frac{d_s - c}{d_f - c}\right) = 0.0059$$

Step 8 – Calculate the stress levels in the prestressing steel, regular steel and CFRP

For 1862 MPa prestressing steel:

$$f_{ps} = \begin{cases} 28500\varepsilon_{ps}, & \text{for } \varepsilon_{ps} \leq 0.0086 \\ 270 - \frac{0.04}{\varepsilon_{ps} - 0.007}, & \text{for } \varepsilon_{ps} \geq 0.0086, \text{ controls} \end{cases}$$

$$\text{So, } f_{ps} = 1758 \text{ MPa}$$

$$\text{For mild steel, } f_s = E_s \varepsilon_s = 1172 \text{ MPa} \geq f_y = 414 \text{ MPa}$$

$$\begin{aligned} \text{So, } f_s &= 413.7 \text{ MPa} \\ \text{For CFRP, } f_{fe} &= 0.5 E_f \varepsilon_{fe} = 266.8 \text{ MPa} \end{aligned}$$

Step 9 – Calculate the internal force resultants and check equilibrium

The strain in concrete at failure can be calculated from strain compatibility as follows:

$$\varepsilon_c = (\varepsilon_{fe} + \varepsilon_{bi}) \left(\frac{c}{d_f - c} \right) = 0.0015$$

Concrete stress block factor may be calculated using ACI 318, as follows:

$$\beta_1 = \frac{4\varepsilon'_c - \varepsilon_c}{6\varepsilon'_c - 2\varepsilon_c} = 0.699$$

where: ε'_c is strain corresponding to f'_c , calculated as:

$$\varepsilon'_c = \frac{1.7f'_c}{E_c} = 0.003$$

Approximate stress block factor may also be calculated based on the parabolic stress-strain relationship for concrete, as follows:

$$\alpha_1 = \frac{3\varepsilon'_c - \varepsilon_c^2}{3\beta_1 \varepsilon_c^2} = 9.591$$

Step 10 – Adjust c until force equilibrium is satisfied

Steps 6 through 9 were repeated several times with different values of c until equilibrium was achieved. The final results are:

$$\begin{aligned} c &= 87.6 \text{ mm}, \varepsilon_{ps} = 0.0097 < 0.035, f_{ps} = 1758 \text{ MPa}, f_s = 414 \text{ MPa}, f_{fe} = 266 \text{ MPa}, \\ \varepsilon_{fe} = \varepsilon_{fd} &= 0.0065, \varepsilon_c = 0.0012, \beta_1 = 0.693, \alpha_1 = 0.515 \end{aligned}$$

Step 11 – Calculate design flexural strength of the section

The design flexural strength is calculated using the equation below. An additional reduction factor, $\psi_f = 0.85$, is applied to the contribution of the FRP system.

$$\Phi M_n = 0.9 \left[A_s f_s \left(d_s - \frac{\beta_1 c}{2} \right) + A_{ps} f_{ps} \left(d_p - \frac{\beta_1 c}{2} \right) + 0.85 A_f f_{fe} \left(d_f - \frac{\beta_1 c}{2} \right) \right] = 301 \text{ kN} \cdot \text{m} \text{ (kN} \cdot \text{m ?)}$$

For a point load on a three point bending and 3.8 m simple span, failure load = 394 kN.

REFERENCES

- [1] ASCE, Report Card on America's Infrastructure, *Infrastructurereportcard.org*, Web. <http://www.infrastructurereportcard.org/bridges/>, 2013.
- [2] AD Miller, *Repair of Impact-Damaged Prestressed Concrete Bridge Girders Using Carbon Fiber Reinforced Polymer (CFRP) Materials*, North Carolina State University, USA, 2006.
- [3] JW Tedesco, JM Stallings and M El-Mihilmy, Rehabilitation of a Reinforced Concrete Bridge Using FRP Laminates, *Final Report, Alabama Department of Transportation*, 1998, 930–341.
- [4] D Yang, BD Merrill, and TE Bradberry, Texas' Use of CFRP to Repair Concrete Bridges. *ACI Special Publication*, 2011, 277, 39-57.
- [5] H Ganga Rao and P Vijay, Bending Behavior of Concrete Beams Wrapped with Carbon Fabric, *Journal of Structural Engineering*, 1998, 124(1), 3–10.
- [6] A J Wolanski, *Flexural Behavior of Reinforced and Prestressed Concrete Beams Using Finite Element Analysis*, Marquette University, USA, 2004.
- [7] AASHTO, Guide Specifications for Design of Bonded FRP Systems for Repair and Strengthening of Concrete Bridge Elements, *Washington, DC: American Association of State Highway and Transportation Officials*, 2012.
- [8] ACI, Guide for the Design and Construction of Externally Bonded FRP Systems for Strengthening Concrete Structures, *ACI 440.2R-08 Michigan*, 2008.
- [9] CNR-DT 200, Guide for the Design and Construction of Externally Bonded FRP Systems for Strengthening Existing Structures, *Italian Advisory Committee on Technical Recommendations for Construction*, Italy, 2004.
- [10] FIB Bulletin 14, Externally Bonded FRP Reinforcement for RC Structures, *The International Federation for Structural Concrete*, Europe, 2001.
- [11] ISIS, Strengthening Reinforced Concrete Structures with Externally-bonded Fiber-reinforced Polymers, *ISIS Canada Design Manuals*. Winnipeg, Manitoba, 2001.
- [12] M Brace, Composite Strengthening System-Engineering Design Guidelines, *Master Builders*, 1998, 1.
- [13] NCHRP, Recommended Guide Specification for the Design of Externally Bonded FRP Systems for Repair and Strengthening of Concrete Bridge Elements. *National Cooperative Highway Research Program*, Report 655, 2010.
- [14] The Concrete Society, Design Guidance for Strengthening Concrete Structures Using Fiber Composite Materials, *TR55*, Surrey, United Kingdom, 2012.
- [15] NCHRP, Determining Highway Maintenance Costs, *National Cooperative Highway Research Program*, Report 688, 2011.

-
- [16] ACI, Building Code Requirements for Structural Concrete, *ACI 318-14*, Farmington Hills, MI, **2014**.
- [17] AASHTO, LRFD Bridge Design Specifications, *American Association of State Highway and Transportation Officials*, Washington, DC, **2014**.
- [18] A ElSafty and M K Graeff, The Repair of Damaged Bridge Girders with Carbon Fiber Reinforced Polymer “CFRP” Laminates, *TRID*, Web. <http://trid.trb.org/view.aspx?id=1224031>, **2012**.
- [19] ANSYS Parametric Design Language (Version 14.5), ANSYS. Canonsburg, Pennsylvania, **2012**.
- [20] M Mohanamurthy, *Prestressed Girder Strengthening using Fiber Reinforced Polymer: Finite Element Modeling and Codal Comparision*, University of Texas at Arlington, USA, **2013**.
- [21] D Kachlakev and D D McCurry, Behavior of Full-Scale Reinforced Concrete Beams Retrofitted for Shear and Flexural with FRP Laminates, *Composites Part B: Engineering*, **2000**, 31(6-7), 445–452.